Available online at www.sciencedirect.com

ScienceDirect

Ceramics International 42 (2016) 7270–7277

CERAMICS INTERNATIONAL

www.elsevier.com/locate/ceramint

Microstructure and electrical conductivity of fast fired Sr- and Mg-doped lanthanum gallate

S.L. Reis*, E.N.S. Muccillo

Energy and Nuclear Research Institute – IPEN, PO Box 11049, S. Paulo 05422-970, SP, Brazil

Received 25 November 2015; received in revised form 12 January 2016; accepted 13 January 2016
Available online 22 January 2016

Abstract

$La_{0.9}Sr_{0.1}Ga_{0.8}Mg_{0.2}O_{3-\delta}$ solid electrolytes were consolidated by fast firing aiming to investigate the effects of the sintering method on densification, microstructure and ionic conductivity. Powder mixtures were prepared by solid state reaction at 1250 and 1350 °C for 12 h, and fast fired at 1450 and 1500 °C temperatures for 5 and 10 min. The content of impurity phases was found to be quite low with this sintering method. Relatively high density (> 90% of the theoretical value) and low porosity (< 1.5%) were readily obtained for powder mixtures calcined at 1250 °C. The activation energy for conduction was approximately 1 eV. Specimens fast fired at 1450 °C for 10 min with a mean grain size of 2.26 μm reached the highest value of total ionic conductivity, 22 mS cm^{-1}, at 600 °C.

Keywords: A: Sintering; C: Electrical conductivity; D: Perovskites; E: Fuel cells

1. Introduction

Lanthanum gallate with partial substitutions by Sr and Mg, $La_{1-x}Sr_xGa_{1-y}Mg_yO_{3-\delta}$ has received considerable attention as a promising solid electrolyte for solid oxide fuel cells operating at intermediate temperatures (600–800 °C), owing to its singular electrical and electrochemical properties [1–7]. Among the several compounds formed by varying the strontium and the magnesium contents, that with $x=0.1$ and $y=0.2$ exhibits a perovskite type crystalline structure with orthorhombic symmetry and has been thoroughly investigated [1, 8, 9]. $La_{0.9}Sr_{0.1}Ga_{0.8}Mg_{0.2}O_{3-\delta}$, hereafter named LSGM, exhibits high ionic conductivity (0.17 S cm^{-1} at 800 °C) and ionic transport number of approximately 1 in a wide range of oxygen partial pressures [1].

The LSGM compound is usually prepared by the solid state method, comprising the mixture of the starting reagents followed by high temperature reaction and conventionally sintered. The product material frequently contains minor amounts of secondary or impurity phases, such as $LaSrGaO_4$, $LaSrGa_3O_7$, $La_4Ga_2O_9$ and MgO [10–12]. The thermodynamic stability and the electrical conductivity of La- and Ga-containing impurity phases and of $La_{0.8}Sr_{0.2}Ga_{0.8}Mg_{0.2}O_{3-\delta}$ have already been investigated [13]. Based on the obtained results, it has been proposed that the ideal sintering temperature should be relatively high (1500 °C) to obtain good densification and because the solubility of strontium and magnesium is maximum at such high temperature, although the relative density seldom exceeds 95% [13]. Moreover, it was suggested the use of a fast cooling rate from the sintering temperature to preserve, as much as possible, the phase composition obtained at high temperature [13].

Relatively few studies may be found, on modified thermal cycles with fast heating and cooling rates during sintering of LSGM. The spark plasma sintering (SPS) technique was found suitable for obtaining LSGM specimens with density in excess of 90% at relatively low temperatures (1200–1300 °C) [14,15], and the use of high pressures allowed for full densification [16]. In addition, the SPS technique was effective to produce

*Correspondence to: Center of Materials Science and Technology, Energy and Nuclear Research Institute – IPEN, PO Box 11049, S. Paulo 05422-970, SP, Brazil. Tel.: +55 11 31339203.
E-mail address: shirley.reis@usp.br (S.L. Reis).

http://dx.doi.org/10.1016/j.ceramint.2016.01.121
0272-8842/

LSGM specimens with grain sizes smaller than 1 μm and with negligible (about 2% or less) impurity phases. In those studies the LSGM powder was synthesized by chemical methods, which are known to give rise to low content of impurity phases. Good densification (~98% of relative density) was also obtained by rapid solidification with CO_2 laser using LSGM powder prepared by the mixing of oxides method [17]. The reported total (grain plus grain boundary) electrical conductivity of LSGM at 600 °C varies considerably from 0.007 [14] to 0.027 S cm^{-1} [17]. Those relatively low values were attributed to the significant blocking of charge carriers at grain boundaries, due to the small grain sizes [14].

Another method applying fast heating and cooling rates, known as fast firing, was originally proposed for obtaining high densification and fine grain materials for ceramics exhibiting high activation energy for densification compared to that for grain growth [18, 19]. In this method, the green compact is heated at a fast rate up to a high temperature, usually higher than that of conventional sintering remaining for short time, and then, it is fast cooled down to room temperature. The fast firing method has been applied to several ceramic materials such as Al_2O_3, $BaTiO_3$, yttria-doped zirconia, manganese-doped ceria and Al_2O_3–TiC composite [18–22]. The main issues of this method of sintering were recently reviewed [23].

In a previous work, we consolidated chemically synthesized powders of LSGM by fast firing [24]. The 90% dense specimens showed negligible impurity phase contents, but relatively low electrical conductivity probably due to limited densification. However, for practical applications, high relative density (≥ 92% of the theoretical value) and suitable electrical conductivity are required. Therefore, in this work, the $La_{0.9}Sr_{0.1}Ga_{0.8}Mg_{0.2}O_{3-\delta}$ compound was prepared by solid state reaction, and green compacts were fast fired at high temperatures aiming to establish sintering parameters for obtaining high densification along with reduced amounts of impurity phases. The effect of the sintering method on the electrical conductivity of LSGM was investigated by impedance spectroscopy measurements.

2. Experimental procedure

2.1. Material preparation

$La_{0.9}Sr_{0.1}Ga_{0.8}Mg_{0.2}O_{3-\delta}$ compound was prepared by the conventional solid state reaction method with La_2O_3 (99.9%, Alfa Aesar), $SrCO_3$ (P. A., Vetec), Ga_2O_3 (99.9%, Alfa Aesar) and MgO (P. A., Vetec) as starting materials. The lanthanum precursor was heat treated at 1000 °C for 3 h prior to use. The starting materials were mixed together in the stoichiometric ratio and calcined at 1250 °C and 1350 °C for 4 h. These temperatures were selected from a previous study [25]. The calcination step was repeated twice with intermediate deagglomeration in an agate mortar to improve the mixing of the powder particles and, consequently, the reaction among the several components. After 12 h of calcination the powder mixture was attrition milled for 1 h in a teflon jar with zirconia balls (ϕ 2 mm) in alcoholic medium. The dried mixture was uniaxially and isostatically (200 MPa) pressed into pellets (ϕ 10 mm and 2–3 mm thickness) without any binder material. Green pellets were introduced in a pre-heated (1450 or 1500 °C) tubular furnace (Lindberg, BlueM). After 5 or 10 min. of isothermal treatment, the pellets were pulled out of the furnace and quickly cooled down in air to room temperature. These experiments were repeated a number of times to ensure reproducibility.

2.2. Characterization methods

The crystalline structure of fast fired pellets was characterized by X-ray diffraction, XRD (Bruker-AXS, D8 Advance) in the 20–80 ° 2θ range with Cu K_α radiation ($\lambda = 1.5405$ Å), and 0.05° step size with 2 s counting time. The main impurity phases were identified with the corresponding ICDD files: 24-1208 ($LaSrGaO_4$), 37-1433 ($La_4Ga_2O_9$) and 45-0637 ($LaSrGa_3O_7$). The XRD patterns were normalized for the most intense reflection of the orthorhombic phase for comparison purpose, once the amount of impurity phases was not quantified. The sintered density was determined by the immersion method with distilled water and compared to the theoretical density (6.67 g cm^{-3}, ICSD 51-288). The porosity of fast fired pellets was estimated according to ASTM C20-00.

The main microstructural features of sintered pellets were studied by field emission scanning electron microscopy, FESEM (FEI, Inspect F50). The mean grain size, G, was determined by the intercept method on a large population of grains. Electrical conductivity measurements were carried out by impedance spectroscopy (HP 4192A) in the 5 Hz–13 MHz frequency and 280–420 °C temperature range, respectively. Silver paste was painted onto parallel surfaces of the pellets and fired at 400 °C to act as electrode. The impedance diagrams were normalized for pellet dimensions for comparison purpose, and the collected data were analyzed in impedance mode with special software [26].

3. Results and discussion

3.1. Structure and microstructure

Fig. 1 shows XRD patterns of LSGM recorded after each processing step for powders calcined at 1250 °C. The diffraction pattern of the powder mixture (PM) is included as reference. After the first calcination step, the diffraction pattern displays the main reflections of LSGM with orthorhombic symmetry according to ICSD 51-288, along with $La_4Ga_2O_9$ (3) and $LaSrGa_3O_7$ (4) as impurity phases, and unreacted La_2O_3 (1) and Ga_2O_3 (2). The most intense reflection, in this pattern belongs to the gallium-rich phase $LaSrGa_3O_7$. The reflections of the LSGM phase attain high intensity after the second calcination step, whereas the fraction of the $LaSrGa_3O_7$ decreases. The reflections of the starting powders are no longer observed after 8 h of calcinations at 1250 °C. In addition, a low intensity reflection belonging to $LaSrGaO_4$ (5) phase is also detected. The third calcination step promotes further

decrease of the intensity of reflections corresponding to $LaSrGa_3O_7$. No other changes are noticed in the XRD pattern obtained after attrition milling. Then, after 12 h of calcination at 1250 °C, the powder mixture is primarily constituted by the orthorhombic LSGM phase. Powder mixtures calcined at 1350 °C exhibit similar behavior, except that after the first calcination step the orthorhombic LSGM is the predominant phase [25].

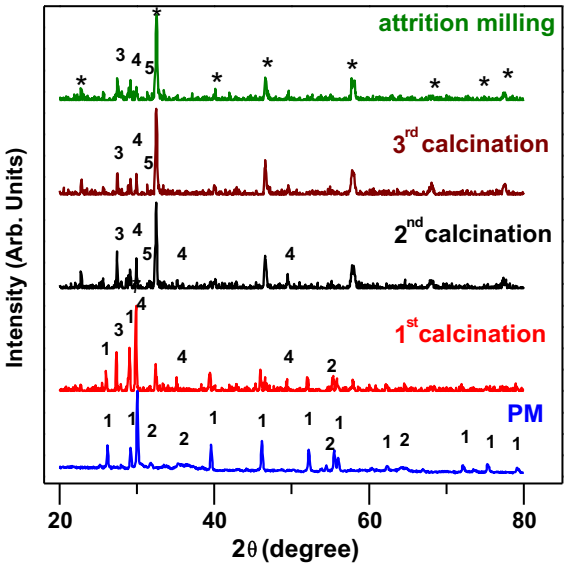

Fig. 1. XRD patterns of the powder mixture (PM) after calcinations at 1250 °C for 4 h and after attrition milling for 1 h. (*) LSGM, (1) La_2O_3, (2) Ga_2O_3, (3) $La_4Ga_2O_9$, (4) $LaSrGa_3O_7$ and (5) $LaSrGaO_4$.

The microstructure of the powder mixture after the processing steps is observed in the FESEM micrographs of Fig. 2. After calcinations at 1250 °C (Fig. 2a, b and c) the powder mixture consists of agglomerated particles. The observed growth of the particle size and neck formation show that the sintering process is underway. This result is in general agreement with that obtained by dilatometry for $La_{0.8}Sr_{0.2}Ga_{0.8}Mg_{0.2}O_{3-\delta}$ [13]. The milling step allowed for obtaining loose particles, despite the difference in their sizes, Fig. 2d. For powder mixtures calcined at 1350 °C, sintering of the particles is even more evident. It should be remarked that high temperatures and longer dwell times are required during calcination to ensure total decomposition of precursors and formation of the orthorhombic phase (see Fig. 1).

Figs. 3 and 4 show XRD patterns of LSGM sintered pellets prepared with powders calcined at 1250 and 1350 °C, respectively.

In Fig. 3a there is a predominance of the LSGM phase for all dwell temperatures and times. The 2θ angular range (25–32°) where the most intense reflections of impurity phases are detected is highlighted in Fig. 3b, revealing that the fraction of these phases is lower in fast fired specimens, especially after sintering at 1450 °C for 10 min.

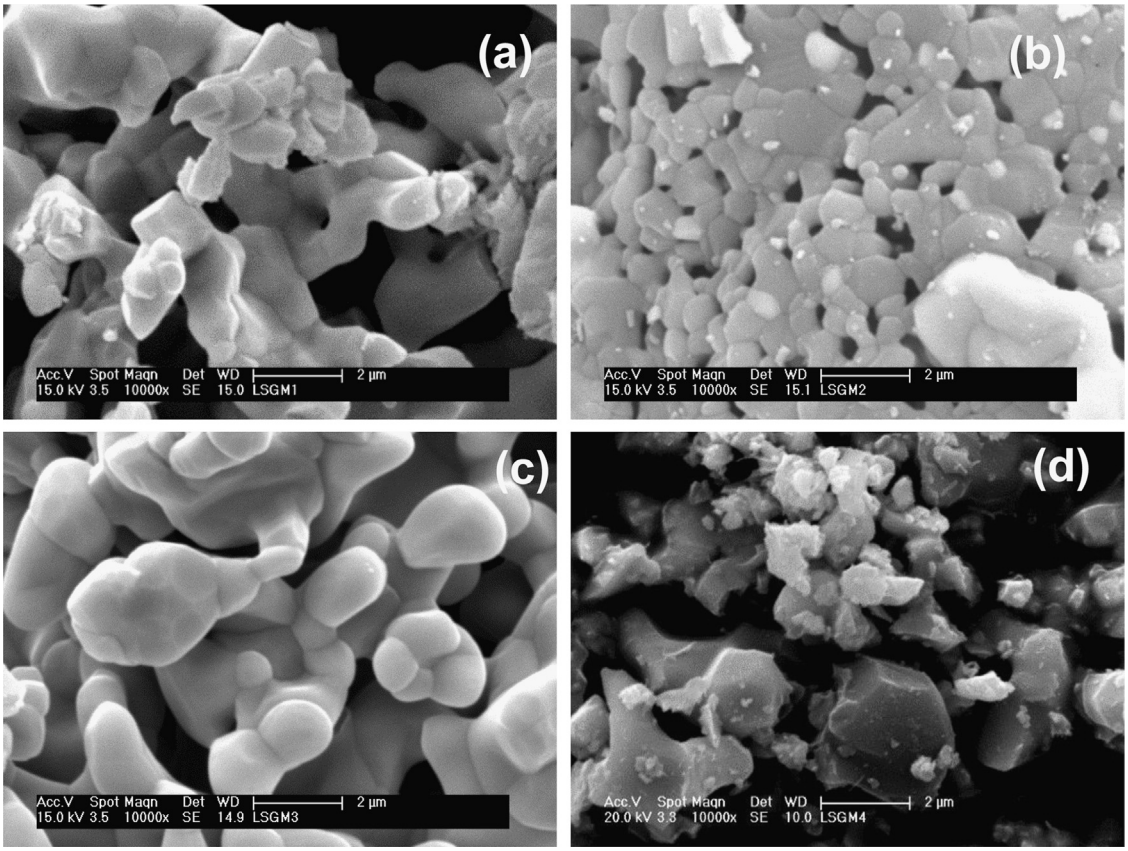

Fig. 2. FESEM micrographs of the powder mixture after (a) first, (b) second and (c) third calcinations at 1250 °C, and (d) attrition milling.

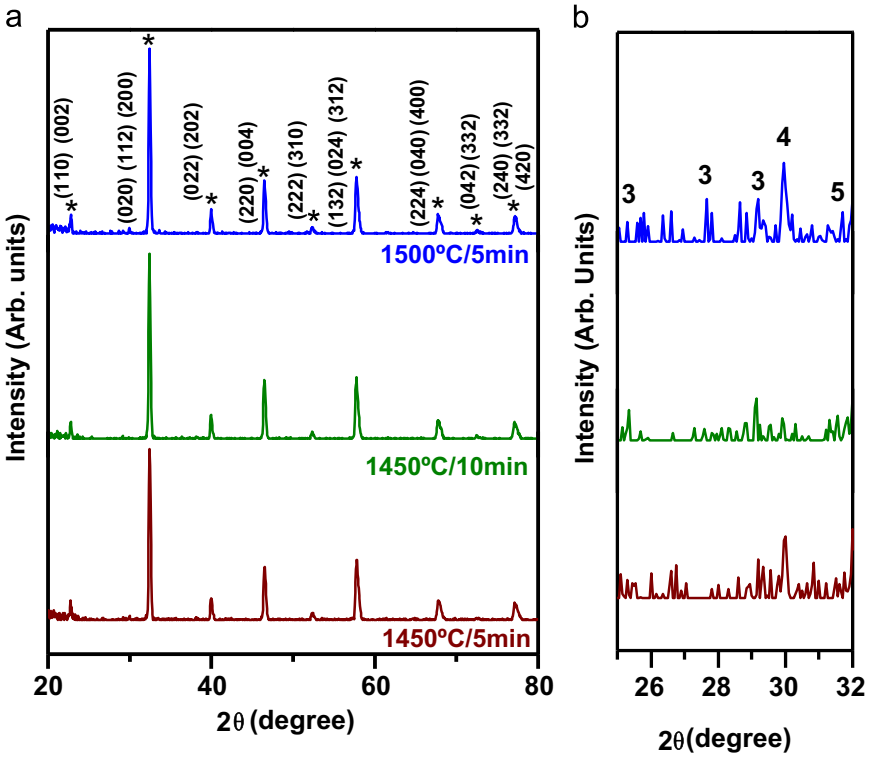

Fig. 3. XRD patterns of fast fired LSGM prepared with powders calcined at 1250 °C in the (a) 20–80° and (b) 25–32° 2θ ranges. (*) LSGM, (3) $La_4Ga_2O_9$, (4) $LaSrGa_3O_7$ and (5) $LaSrGaO_4$.

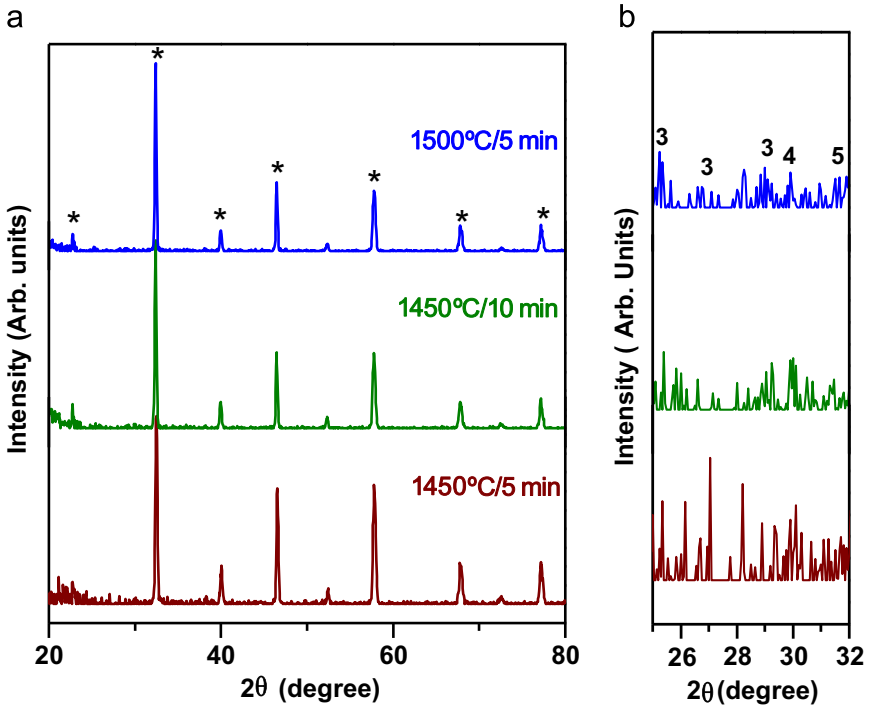

Fig. 4. XRD patterns of fast fired LSGM prepared with powders calcined at 1350 °C in the (a) 20–80° and (b) 25–32° 2θ ranges. (*) LSGM, (3) $La_4Ga_2O_9$, (4) $LaSrGa_3O_7$ and (5) $LaSrGaO_4$.

The XRD patterns of sintered pellets prepared with the powder mixture calcined at 1350 °C (Fig. 4) show similar features as those in Fig. 3, with slight lower content of $LaSrGa_3O_7$ comparing to other impurity phases. It is worth-noting that in these patterns there is no evidence of unreacted MgO, as expected [27].

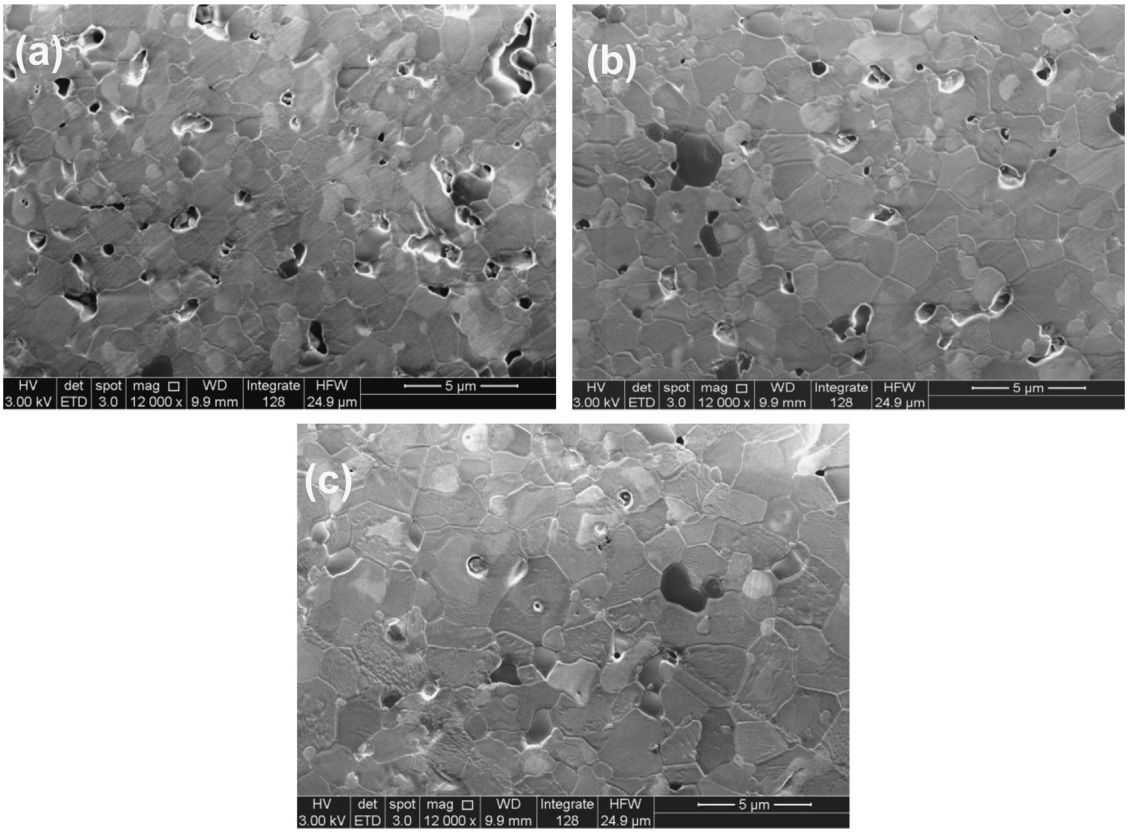

Fig. 5. FESEM micrographs of LSGM pellets prepared with powders calcined at 1250 °C and fast fired at (a) 1450 °C for 5 min, (b) 1450 °C for 10 min, and (c) 1500 °C for 5 min.

A careful microstructure observation was carried out recording several microregions along the cross section and the thickness of the pellets. This procedure was adopted seeking for possible heterogeneities in the microstructure of LSGM caused by differential shrinkage, which may occur during fast firing [23]. In this case, all pellets displayed a homogeneous microstructure, free of microcracks and with uniform distribution of grains.

Fig. 5 shows representative micrographs of fast fired specimens prepared with powder mixtures calcined at 1250 °C. Most of the grains have polygonal shape with wide distribution of sizes. The porosity degree decreases with increasing the annealing temperature and time. Isolated MgO is observed as dark grains, as indicated by arrows in Fig. 5b and c. These microstructure features seem to be characteristic of this compound not depending on the method of sintering [6, 7, 24].

Values of the mean grain size determined by the intercept method, relative density and apparent porosity are listed in Table 1. The mean grain size increases with both the annealing temperature and time. In addition, the mean grain size increases with increasing the calcination temperature, as further evidence of the sintering of powder particles during calcinations at high temperatures.

Good densification and comparatively low apparent porosity were obtained in pellets prepared with the powder mixture calcined at 1250 °C (Table 1), showing the important influence of the processing step in the final microstructure of LSGM.

Table 1
Values of the mean grain size, relative density and apparent porosity of pellets prepared with powder mixtures calcined at 1250 and 1350 °C.

Calcination temperature (°C)	Sintering temperature/ time (°C/min)	Mean grain size (µm)	Relative density (%)	Apparent porosity (%)
1250	1450/5	1.95 ± 0.05	91	1.30
	1450/10	2.26 ± 0.05	93	0.60
	1500/5	2.77 ± 0.07	95	0.66
1350	1450/5	3.19 ± 0.08	78	24.4
	1450/10	3.35 ± 0.09	82	15.6
	1500/5	4.07 ± 0.08	84	15.1

3.2. Impedance spectroscopy

Electrical conductivity measurements were carried out by impedance spectroscopy on fast fired pellets of LSGM with high density, i.e., those prepared with the powder mixture calcined at 1250 °C. Typical $-Z''(\omega)$ x $Z'(\omega)$ diagrams of LSGM measured at 340 °C are shown in Fig. 6. Numbers on top of experimental points stand for the logarithm of the relaxation frequency (in Hz). The high-frequency and the intermediate-frequency arcs are ascribed to the bulk (or grain) resistance and capacitance, and to the grain boundary blocking effect, respectively. The latter partially overlaps the low-frequency arc due to reactions at the electrolyte/electrode

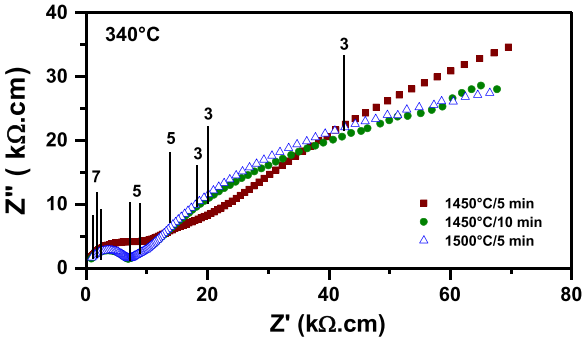

Fig. 6. Impedance spectroscopy spectra of fast fired LSGM pellets measured at 340 °C. Numbers over experimental points are the logarithm of the frequency (in Hz).

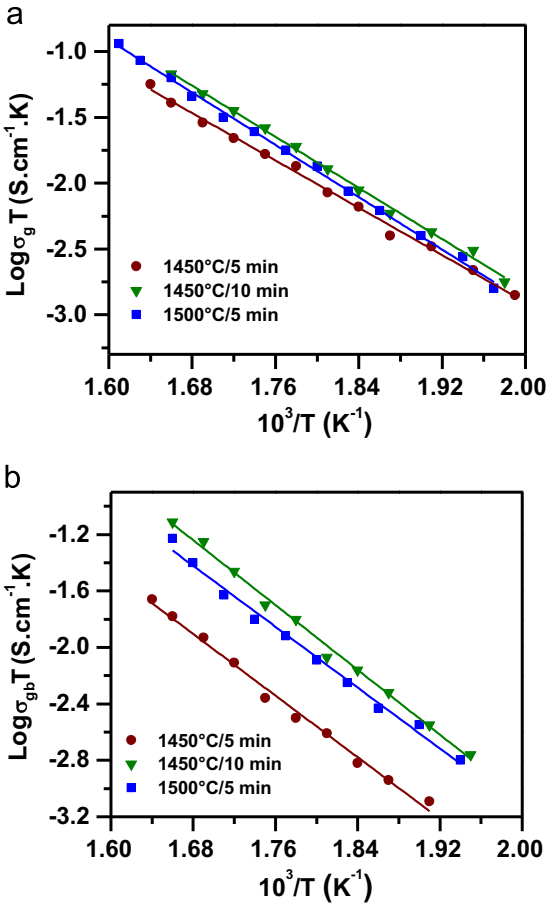

Fig. 7. Arrhenius plots of (a) grain and (b) grain boundary conductivities of fast fired LSGM.

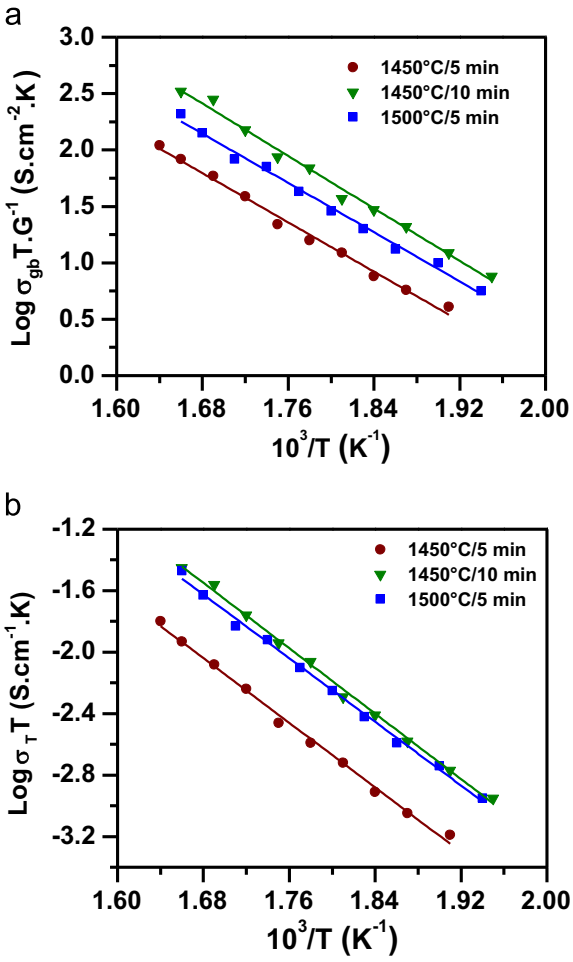

Fig. 8. Temperature dependence of the total ionic conductivity of fast fired LSGM.

interface. The arc centers fall below the real axis as usual for oxide-ion conductors. The off-axis angles are ~14° (high-frequency) and ~20° (intermediate-frequency). In the whole temperature range of measurements these two arcs could be well deconvoluted in frequency and the ionic conductivity of grains and grain boundaries be evaluated.

Fig. 7a and b shows Arrhenius plots of grain conductivity and grain boundary blocking effect, respectively. The grain conductivity, σ_g (Fig. 7a), is slightly lower for LSGM pellets fast fired at 1450 °C for 5 min. This effect may be ascribed to comparatively lower grain homogeneity of this specimen. In fact, high homogeneity grains are expected to be formed at higher temperatures (~1500 °C), when the solubility of strontium and magnesium is maximized [13]. The grain conductivity of LSGM pellets sintered at 1450 °C for 10 min and 1500 °C for 5 min are similar within experimental errors.

The grain boundary conductivity, σ_{gb} (Fig. 7b) of LSGM sintered at 1450 °C for 5 min is about half-order of magnitude lower than that of pellets sintered at 1450 °C for 10 min. This large difference in ionic conductivity at the grain boundary region evidences high heterogeneity in the interface compared to the bulk of LSGM specimens. Surprisingly, the highest grain boundary conductivity is exhibited by specimens sintered at 1450 °C for 10 min.

Fig. 8a depicts the grain boundary conductivity of fast fired LSGM after normalization taken into account the mean grain size. The difference of the grain boundary conductivity between specimens sintered for 5 and 10 min at 1450 °C remains approximately half-order of magnitude. This means that the difference in the mean grain size may not account for that effect. Similarly, the difference between the grain boundary blocking effect of specimens fast fired at 1450 °C for 10 min and 1500 °C for 5 min may not be attributed to

Table 2
Values of the activation energy, and total electrical conductivity at 360 (σ^{360}) and 600 °C (σ^{600}) of fast fired LSGM prepared with the powder mixture calcined at 1250 °C.

Sintering temperature/time (°C/min)	Activation energy (eV)	[a]σ^{360} (10^{-2} mS cm^{-1})	[b]σ^{600} (mS cm^{-1})
1450/5	1.04 ± 0.05	4.8	6
1450/10	1.05 ± 0.05	14.9	22
1500/5	1.01 ± 0.05	12.6	16

[a]Measured.
[b]Estimated values.

variation of the interface area. It is generally known that reduction of gallium oxides readily occurs at high temperatures and under reducing atmospheres with formation of volatile Ga_2O [28]. This loss of gallium at high temperatures leads to deviation of stoichiometry and consequent decrease of the ionic conductivity. This result reveals that this effect starts at the grain boundaries.

The Arrhenius plots of the total ionic conductivity, σ_T, of fast fired LSGM is show in Fig. 8b. In the limited temperature range of measurements the ionic conductivity shows a linear behavior with activation energy of approximately 1 eV (Table 2). Values of the total ionic conductivity determined at 360 °C and estimated by means of linear interpolation at 600 °C are summarized in Table 2. The total ionic conductivity value at 600 °C for the optimized sintered profile of 1450 °C for 10 min is 22 mS cm^{-1}, in good agreement with the best reported value [17] for LSGM specimens sintered by a fast thermal cycle.

4. Conclusions

The method of fast firing was successfully applied to $La_{0.9}Sr_{0.1}Ga_{0.8}Mg_{0.2}O_{3-\delta}$ compound. High densification was obtained at short times at the annealing temperature for green compacts prepared with powder mixtures calcined at 1250 °C. The sintered specimens exhibit uniform microstructure and low porosity. A suitable choice of the annealing temperature allowed for minimization of gallium loss resulting in specimens with high total ionic conductivity.

Acknowledgments

The authors acknowledge FAPESP (Procs. 96/09604-9 and 2013/07296-2), CNPq (Proc. 304073/2014-8) and CNEN for financial supports. One of the authors (S.L.Reis) is grateful to CNPq (Proc. 505980/2013-4) for the scholarship.

References

[1] T. Ishihara, H. Matsuda, Y. Takita, Doped $LaGaO_3$ perovskite-type oxide as a new oxide ionic conductor, J. Am. Chem. Soc. 116 (1994) 3801–3803.
[2] M. Feng, J.B. Goodenough, A superior oxide-ion electrolyte, Eur. J. Solid State Inorg. Chem. 31 (1994) 663–672.
[3] R. Maric, S. Ohara, T. Fukui, H. Yoshida, M. Nishimura, T. Inagaki, K. Miura, Solid oxide fuel cells with doped lanthanum gallate electrolyte and $LaSrCoO_3$ cathode, and Ni-samaria-doped ceria cermet anode, J. Electrochem. Soc. 146 (1999) 2006–2010.
[4] T. Ishihara, T. Shibayama, M. Honda, H. Nishiguchi, Y. Takita, Intermediate temperature solid oxide fuel cells using $LaGaO_3$ electrolyte II. Improvement of oxide ion conductivity and power density by doping Fe for Ga site of $LaGaO_3$, J. Electrochem. Soc. 147 (2000) 1332–1337.
[5] Y. Lin, S.A. Barnett, Co-firing of anode-supported SOFCs with thin $La_{0.9}Sr_{0.1}Ga_{0.8}Mg_{0.2}O_{3-\delta}$ electrolytes, Electrochem. Solid State Lett. 9 (2006) A285–A288.
[6] F. Bozza, R. Polini, E. Traversa, High performance anode-supported intermediate temperature solid oxide fuel cells (IT-SOFCs) with $La_{0.8}Sr_{0.2}Ga_{0.8}Mg_{0.2}O_{3-\delta}$ electrolyte films prepared by electrophoretic method, Electrochem. Commun. 11 (2009) 1680–1683.
[7] N. Yang, A. D'Epifanio, E. Di Bartolomeo, C. Pugnalini, A. Tebano, G. Balestrino, S. Licoccia, $La_{0.8}Sr_{0.2}Ga_{0.8}Mg_{0.2}O_{3-\delta}$ thin films for IT-SOFCs: microstructure and transport properties, J. Power Sources 222 (2013) 10–14.
[8] M. Lerch, H. Boyse, T. Hanse, high-temperature neutron scattering investigation of pure and doped lanthanum gallate, J. Phys. Chem. Solids 62 (2001) 445–455.
[9] P. Datta, P. Majewski, F. Aldinger, Structural studied of Sr- and Mg-doped $LaGaO_3$, J. Alloy Compd. 438 (2007) 232–237.
[10] S. Li, B. Bergman, Doping effect on secondary phases, microstructure and electrical conductivities of $LaGaO_3$ based perovskites, J. Eur. Ceram. Soc. 29 (2009) 1139–1146.
[11] F. Zheng, R.K. Bordia, L.R. Pederson, Phase constitution in Sr and Mg doped $LaGaO_3$ system, Mater. Res. Bull. 39 (2004) 141–155.
[12] P. Majewski, M. Rozumek, F. Aldinger, Phase diagram studies in the systems La_2O_3-SrO-MgO-Ga_2O_3 at 1350–1400 °C in air with emphasis on Sr and Mg substituted $LaGaO_3$, J. Alloy Compd. 329 (2001) 253–258.
[13] M. Rozumek, P. Majewski, F. Aldinger, K. Künstler, G. Tomandl, Preparation and electrical conductivity of common impurity phases in (La,Sr)(Ga,Mg)O_3 solid electrolytes, Ber. DKG 80 (2003) E35–E40.
[14] B. Liu, Y. Zhang, $La_{0.9}Sr_{0.1}Ga_{0.8}Mg_{0.2}O_{3-\delta}$ sintered by spark plasma sintering (SPS) for intermediate temperature SOFC electrolyte, J. Alloy Compd. 458 (2008) 383–389.
[15] H. Borodianska, P. Badica, T. Uchikoshi, Y. Sakka, Q. Vasylkiv, Nanometric $La_{0.9}Sr_{0.1}Ga_{0.8}Mg_{0.2}O_{3-\delta}$ ceramic prepared by low-pressure reactive spark-plasma-sintering, J. Alloy Compd. 509 (2011) 2535–2539.
[16] F. Maglia, U. Anselmi-Tamburini, G. Chiodelli, H.E. Çamurlu, Z. A. Munir, Electrical, structural, and microstructural characterization of nanometric $La_{0.9}Sr_{0.1}Ga_{0.8}Mg_{0.2}O_{3-\delta}$ (LSGM) prepared by high-pressure spark plasma sintering, Solid State Ion. 180 (2009) 36–40.
[17] J. Zhang, E.J. Liang, X.H. Zhang, Rapid synthesis of $La_{0.9}Sr_{0.1}Ga_{0.8}Mg_{0.2}O_{3-\delta}$ electrolyte by a CO_2 laser and its electric properties for intermediate temperature solid state oxide full cells, J. Power Sources 195 (2010) 6758–6763.
[18] M.P. Harmer, R.J. Brook, Fast firing-microstructural benefits, J. Br. Ceram. Soc. 80 (1981) 147–148.
[19] H. Mostaghaci, R.J. Brook, Production of dense and fine grain size $BaTiO_3$ by fast firing, Trans. J. Br. Ceram. Soc. 82 (1983) 167–170.
[20] D.H. Kim, C.H. Kim, Effect of heating rate on pore shrinkage in yttria-doped zirconia, J. Am. Ceram. Soc. 76 (1993) 1877–1878.
[21] G.J. Pereira, R.H.R. Castro, D.Z. de Florio, E.N.S. Muccillo, D. Gouvea, Densification and electrical conductivity of fast fired manganese-doped ceria ceramics, Mater. Lett. 59 (2005) 1195–1199.
[22] M. Lee, M.P. Borom, L.E. Szala, Rapid rate sintering of ceramics, US Patent 4490319, 1984.
[23] D.E. Garcia, S.N. Klein, D. Hotza, Advanced ceramics with dense and fine-grained microstructures through fast firing, Rev. Adv. Mater. Sci. 30 (2012) 273–281.
[24] S.L. Reis, E.N.S. Muccillo, Ionic conductivity of chemically synthesized $La_{0.9}Sr_{0.1}Ga_{0.8}Mg_{0.2}O_{3-\delta}$ solid electrolyte, Adv. Mater. Res. 975 (2014) 81–85.

[25] S.L. Reis, E.N.S. Muccillo, Effect of attrition milling and calcination temperature on phase composition of strontium- and magnesium-doped lanthanum gallate, Mater. Sci. Forum 727–728 (2012) 516–521.

[26] M. Kleitz, J.H. Kennedy, In: P. Vashishta J.N. Mundy G.K. Shenoy (Eds.), Fast ion transport in solids, electrodes and electrolytes, 1979 North-Holland, Amsterdam, pp. 185–186.

[27] R. Polini, A. Pamio, E. Traversa, Effect of synthetic route on sintering behaviour, phase purity and conductivity of Sr- and Mg-doped $LaGaO_3$ perovskiques, J. Eur. Ceram. Soc. 24 (2004) 1365–1370.

[28] K. Yamaji, T. Horita, M. Ishikawa, N. Sakai, H. Yokokawa, Chemical stability of the $La_{0.9}Sr_{0.1}Ga_{0.8}Mg_{0.2}O_{2.85}$ electrolyte in a reducing atmosphere, Solid State Ion. 121 (1999) 217–224.